diverged, collimated, passed through a transparency, and the resulting diffraction pattern (optical transform) was imaged on the far side by a plus lens. An enlarged image of the transform was cast on a distant rear projection screen by a final lens and photographed there with Polaroid P/N 55 film. Transforms of the grating strips (Fig. 2, D and E) were prepared simultaneously to provide a reference scale in spatial frequency space. The power spectra of the cones are shown in the right column of Fig. 1. Figure $1A_3$ shows the spectrum of the central fovea, which consists of a delta function at the origin surrounded by a circular island of empty space whose radius is on the order of 110 cycle/deg (*9*). Figure 2 illustrates the spectral consequencies of sampling with an array having a spectrum of this general form. Spatial frequencies less than half the radius of the noise-free island escape masking by noise, whereas higher frequencies are scattered into broadband noise containing energy at all spatial orientations (*10*). For an array of cones whose Nyquist frequency would be N cycle/deg if arranged in a spatial lattice (such as square or hexagonal; N would be essentially the same for both) the optimal radius for a noise-free island would be $2N$ cycle/deg. Young's cell count for the rhesus foveola is 19.4 cones per 100 μm^2 (*7*), which implies a nominal Nyquist frequency of 53 cycle/deg or a noise-free island radius of 106 cycle/deg. The spectra of the parafovea (Fig. $1B_3$) and periphery (Fig. $1C_3$) follow the same circular noise-free island pattern as the fovea, and there is a similar agreement between the radius of the islands (approximately 30 cycle/deg for the parafovea and 18 cycle/deg for the periphery); the optimal $2N$ values implied by the nominal Nyquist limits for these regions (28 cycle/deg for the parafovea, based on a cell count of 1.4 cones per 100 μm^2; and 19 cycle/deg for the periphery, based on a cell count of 0.6 cones per 100 μm^2). The spectrum of the far periphery (Fig. $1D_3$) also suggests the same pattern, but here the resolution limits of the apparatus (approximately 5 cycle/deg) would obscure a noise-free island at the optimal radius of 7 cycle/deg (0.3 cones per 100 μm^2).

Computer simulation combined with optical transform analysis shows that desert island spectra like those of the cones are characteristic of "Poisson disk" arrays—points scattered in the plane according to a Poisson distribution, but subject to the restriction of a fixed minimum distance between each point and its nearest neighbor (*11*). It seems possible that sampling arrays constructed on this basis might be useful in artificial image recording systems.

JOHN I. YELLOTT, JR.
Cognitive Science Group,
School of Social Sciences,
University of California, Irvine 92717

References and Notes

1. J. C. Dainty and R. Shaw, *Image Science* (Academic Press, London, 1974); D. E. Pearson, *Transmission and Display of Pictorial Information* Wiley, New York, 1975).
2. F. W. Campbell and R. W. Gubisch, *J. Physiol. (London)* **197**, 558 (1966); R. W. Gubisch, *J. Opt. Soc. Am.* **57**, 407 (1967); J. A. M. Jennings and W. N. Charman, *Vision Res.* **21**, 445 (1981).
3. G. Osterberg, *Acta Ophthalmol. Suppl.* **6**, 11 (1935); S. L. Polyak, *The Vertebrate Visual System* (Univ. of Chicago Press, Chicago, 1957); J. Yellott, B. Wandell, T. Cornsweet, in *Handbook of Physiology*, section 1, vol. 3, *Sensory Processes*, I. Darian-Smith, Ed. (American Physiological Society, Bethesda, Md., in press).
4. H. Wässle and H. T. Rieman, *Proc. R. Soc. London Ser. B* **200**, 441 (1978).
5. J. W. Goodman, *Introduction to Fourier Optics* (McGraw-Hill, New York, 1968); D. Nagel, *J. Opt. Soc. Am.*, in press.
6. P. F. Scott, *Distribution and Estimation of the Autocorrelation Function of a Randomly Sampled Signal* (Report No. 76 CRD 180, General Electric, Schenectady, N.Y., 1976).
7. R. W. Young, *J. Cell Biol.* **49**, 303 (1971), figures 10, 12, 14, and 16.
8. G. Harburn, C. A. Taylor, T. R. Welberry, *Atlas of Optical Transforms* (Cornell Univ. Press, Ithaca, 1975).
9. The same spectrum is also found in the human fovea [J. Yellott, *Vision Res.* **22**, 1205 (1982)]. No comparable analysis of extrafoveal human retina has yet been made. In general, however, human and rhesus eyes seem to be alike in all respects, and one would expect human results to be the same as those reported here for rhesus.
10. D. R. Williams and R. Collier [*Science* **221**, 385 (1983)] have shown that this scattered noise can mediate forced choice psychophysical discriminations between uniform fields and gratings at spatial frequencies much higher than the nominal Nyquist limits implied by receptor density.
11. J. I. Yellott, Jr., *Invest. Ophthalmol. Visual Sci.* **24** (Suppl. 3), 147 (Abstr.) (1983).

12. I thank P. Channing, T. Batey, M. Rudd, and J. W. Yellott for technical help; A. Ahumada, D. Nagel, and D. Williams for valuable discussions; and R. W. Young for permission to reproduce the photomicrographs in Fig. 1. Supported by a faculty research fellowship from the University of California, Sloan Foundation grant 80-6-12 to the UCI Cognitive Science Group, and National Aeronautics and Space Administration grant NCA2-OR345-301.

14 March 1983

Consequences of Spatial Sampling by a Human Photoreceptor Mosaic

Abstract. *The short wavelength color mechanism in the human visual system can distinguish gratings from uniform fields of the same average radiance at spatial frequencies that are twice as high as the highest at which it can resolve bars in the grating. This discrimination above the resolution limit is associated with a splotchy or mottled appearance of the grating similar to two-dimensional noise. The most plausible explanation for the mottled pattern is that it is a moiré pattern produced by aliasing (spatial undersampling) by an irregular and sparse mosaic of short wavelength cones.*

The design of imaging systems that discretely sample a continuous waveform is constrained by the problem of aliasing; if the sampling points are not close enough, high frequencies can masquerade in the reconstructed waveform as low frequencies (*1*). This constraint also applies to biological imaging systems: the mosaic of photoreceptors samples the retinal image. Indeed, there is behavioral evidence for aliasing by the regular ommatidial arrays in insect compound eyes (*2*). We now report evidence for aliasing in the human visual system when high-frequency gratings are seen via the mosaic of short wavelength [blue-sensitive (B)] cones.

Observers viewed a 10° violet grating superimposed on a 580-nm, 13.3° background intended to isolate the B mechanism (*3*). The axial chromatic aberration of the eye was compensated for by adjusting the optical distance of the violet grating relative to the fixated yellow background. Gratings were presented for 500 msec every third second. Between presentations, the grating was replaced by a uniform violet field that was coextensive with the grating and had the same average radiance. For each in a series of grating radiances, observers made two kinds of settings: they adjusted the grating spatial frequency until they could just detect the presence of bars in the target, and until they could just discriminate the grating from the uniform field that replaced it.

Consistent with the best earlier measures of B mechanism resolution (*4*), the acuity of two observers rose to about 10 and 14 cycle/deg (Fig. 1, A and B). At the highest radiance, one observer could distinguish between the grating and the uniform field at a spatial frequency of 23 cycle/deg and the other at 35 cycle/deg, more than twice the highest frequencies at which they could resolve bars. Similarly, a third, naïve observer (not shown) could resolve bars up to 11 cycle/deg yet could distinguish gratings from uniform fields up to 25 cycle/deg (*5*). As spatial frequency was increased at high grating

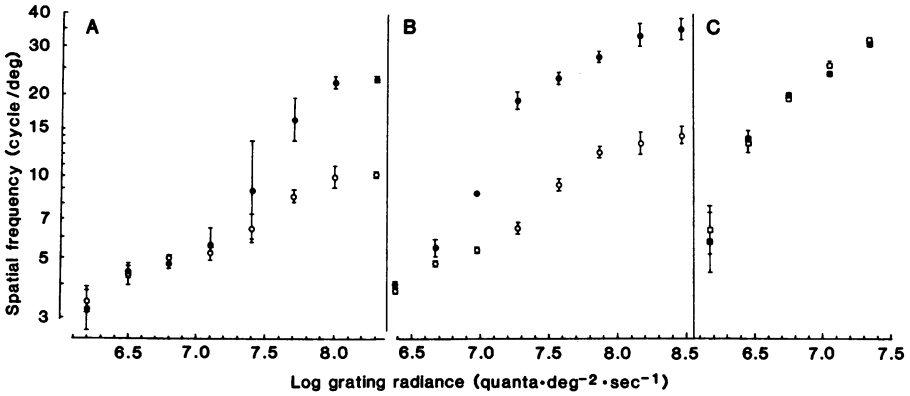

Fig. 1. (A) B mechanism acuity for observer M.M. Open circles represent the highest spatial frequency of a 420-nm grating at which the observer could resolve bars; closed circles represent the highest spatial frequency at which he could distinguish the grating from a uniform field of the same average radiance, as a function of radiance of the grating field. The grating was superimposed on a 580-nm background field. Error bars represent one standard error of the mean calculated from between-session variability. (B) B mechanism acuity for observer D.R.W. The grating and uniform field were 440 nm. (C) G mechanism acuity for D.R.W. The grating was superimposed on 10 log quanta deg^{-2} sec^{-1}, 420-nm background instead of yellow background.

radiances, observers reported that the bar pattern began to break up, giving way to a mottled or splotchy pattern resembling two-dimensional noise. This nonoriented pattern changed rapidly over time. At still higher frequencies, the mottled pattern disappeared and the exchange between grating and uniform field could not be detected.

This mottled pattern originates in the visual system, not in our apparatus. Observers reported that the splotchy pattern changed rapidly over time; yet the fields produced by the apparatus are static. Also, spectral sensitivity measurements show that the mottled pattern is confined to gratings seen via B cones (at least for spatial frequencies less than 35 cycle/deg, the highest used here). Figure 2 shows the highest spatial frequency that could be distinguished from the uniform field for various wavelengths of the exchanged fields superimposed on a fixed radiance background. The agreement among data for wavelengths of 500 nm and shorter, when plotted with π_3 equivalent units on the abscissa, suggests that the action spectrum for detection of the mottled pattern is that of the B mechanism (*6*). When the middle wavelength [green-sensitive (G)] mechanism intrudes as in the case of the 540-nm grating and uniform field, the splotchy pattern is not seen near the resolution limit; as spatial frequency increases, the last thing seen is the grating itself.

But the eye contains structures other than B cones that absorb short wavelengths, such as the dense network of retinal blood vessels; the mottled pattern could be a moiré pattern produced when a grating is imaged on them. Since the blood vessels lie in front of the photoreceptive layer, if they are responsible for the mottled pattern, it should be visible when a different cone mechanism than the B mechanism detects the stimulus. The detection mechanism can be shifted from the B mechanism to the G mechanism while keeping the grating wavelength fixed by changing the background from 580 to 420 nm. Unlike detection by the B mechanism, we found no intermediate frequency range in which the mottled pattern, but no bars, could be observed (Fig. 1C); this result tends to exclude hypotheses based on prereceptoral filtering as well as apparatus artifacts. This conclusion is supplemented by the observation that the mottled pattern persists when a fixated 1° grating field, seen via B cones, falls within the avascular region of the central fovea (*7*) but still excites B cones surrounding the tritanopic area (*8*).

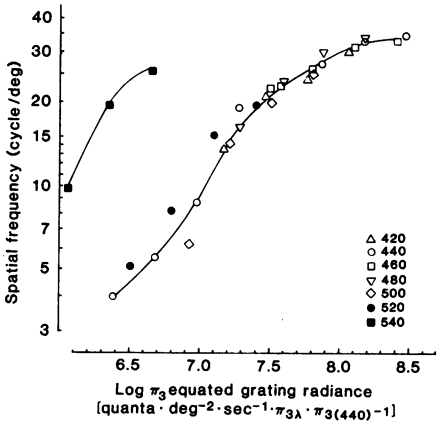

Fig. 2. Highest spatial frequency at which the grating could be discriminated from a uniform field of equal space-averaged radiance as a function of grating radiance (expressed in units equated for Stiles's π_3 mechanism). Different symbols represent different grating wavelengths, all superimposed on the same 580-nm background. Observer, D.R.W.

Though prereceptoral explanations for this mottled pattern have been rejected experimentally, explanations based on postreceptoral mechanisms have not. However, evidence that the origin of the effect lies in the photoreceptor mosaic comes from analyses of its spatial sampling properties. Yellott has studied the sampling properties of cone mosaics, considering the three cone types together, with an optical transform technique (*9*). We have borrowed Yellott's technique to analyze the primate B cone mosaic by itself (*10*).

The selective staining of B cones in the baboon (*11*) and in the monkey (*10, 12*) has revealed that the primate B cone mosaic is not a perfect lattice, though neither is it completely random (*10, 13*). Mosaics of this kind produce moiré patterns containing a broad range of spatial frequencies at all orientations, consistent with the nonoriented, mottled appearance of the pattern observed psychophysically. The B cone mosaic is expected to produce a moiré pattern containing the lowest spatial frequencies, and therefore the moiré pattern should be most visible when the spatial frequency of the grating is roughly the reciprocal of the average receptor spacing. Estimates of B cone spacing in the retinal region beneath the 10° grating (excluding the very center of the fovea) range from 3.5 minutes in baboon (*11*) to roughly 10 minutes estimated psychophysically in the human (*14*), implying that the moiré pattern would be most visible at frequencies in the range from about 6 to 17 cycle/deg. Observations of the mottled pattern suggest that it is most visible at about 8 to 10 cycle/deg, within the expected range. At grating frequencies that are much higher or lower than the reciprocal of the average receptor spacing, the expected moiré pattern contains energy only at high spatial frequencies, those perhaps too high to be resolved by postreceptoral mechanisms. This is consistent with the observation that the mottled pattern is not visible at very low and high grating frequencies. Furthermore, the moiré pattern is expected to change depending on the position of the grating relative to the mosaic; the observed mottled pattern changes rapidly over time, presumably as eye movements shift the retina relative to the image.

Once aliasing has crept into the visual system by photoreceptor undersampling, it is difficult to remove without removing the signal with it. For example, pooling receptor signals after the sampling pro-

cess could selectively filter out the high spatial frequencies responsible for aliasing but not the low-frequency alias they have already spawned. These high frequencies that are not themselves resolved can still leave a clue to their existence in the moiré patterns they produce. One solution to the aliasing problem is to remove the offending spatial frequencies from the image prior to the sampling process. Low-pass optical filtering tends to protect human foveal vision in this way (*15*). Yellott (*9*) has pointed out a second way the visual system copes with aliasing: the irregularity of the cone mosaic smears aliased energy into a broad range of spatial frequencies and orientations, making it less easy to detect. Though spatial vision through the B cone mosaic must also benefit from sampling irregularity, our experiments show that the spurious energy produced by photoreceptor undersampling in one's own retinal mosaic can be visualized.

DAVID R. WILLIAMS
ROBERT COLLIER

Center for Visual Science,
University of Rochester,
Rochester, New York 14627

References and Notes

1. E. T. Whittaker, *Proc. R. Soc. Edinburgh Sect. A* **35**, 181 (1915); C. E. Shannon, *Proc. IRE* **37**, 10 (1949).
2. L. Von Gavel, *Z. Vgl. Physiol.* **27**, 80 (1939); B. Hassenstein, *ibid.* **33**, 301 (1951).
3. Background radiance was 11.4 log quanta deg^{-2} sec^{-1}. The variable frequency, sinusoidal grating, seen in Maxwellian view, was a high-contrast, spatially filtered, moiré fringe pattern produced by sandwiching two 113 cycle/deg Ronchi rulings together. Refractive errors were corrected. Mydriacyl was used to reduce fluctuations of accommodations for one observer (D.R.W.).
4. J. D. Mollon, *Doc. Ophthalmol.* **33**, 87 (1982); C. F. Stromeyer, K. Kranda, C. E. Sternheim, *Vision Res.* **18**, 427 (1978).
5. These results were confirmed with two alternative forced-choice experiments measuring discrimination of horizontal and vertical gratings and discrimination of gratings from uniform fields as a function of spatial frequency. Additional experiments confirmed that the observers were not using a brightness mismatch between the grating and the uniform field to mediate discrimination.
6. G. Wyszecki and W. S. Stiles, *Color Science* (Wiley, New York, 1967), p. 579. The simplifying assumption is made in this report that π_3 and π_4 represent the action spectrum of the B and G cones, respectively.
7. S. L. Polyak, *The Retina* (Univ. of Chicago Press, Chicago, 1941).
8. D. R. Williams, D. I. A. MacLeod, M. Hayhoe, *Vision Res.* **21**, 1341 (1981).
9. J. I. Yellott, Jr., *ibid.* **22**, 1205 (1982); *Science* **221**, 382 (1983). See also A. S. French *et al.*, *Biol. Cybern.* **27**, 229 (1977); D. C. Nagel, paper presented at the annual meeting of the Association for Research in Vision and Ophthalmology, Sarasota, Fla. (1981).
10. D. R. Williams, R. Collier, B. J. Thompson, *Colour Vision: Physiology and Psychophysics*, J. D. Mollon and L. T. Sharpe, Eds. (Academic Press, London, 1983). The pattern of receptors in the B cone mosaic and its optical transform resemble those obtained by Yellott (*9*) for the mosaic of cones taken as a whole, except that the average spacing of B cones is much greater.
11. R. E. Marc and H. G. Sperling, *Science* **196**, 454 (1977).
12. F. M. de Monasterio, S. J. Schein, E. P. McCrane, *ibid.* **213**, 1278 (1981).
13. M. B. Shapiro, S. J. Schein, E. P. McCrane, paper presented at the annual meeting of the Association for Research in Vision and Ophthalmology, Sarasota, Fla. (1982).
14. D. R. Williams, D. I. A. MacLeod, M. M. Hayhoe, *Vision Res.* **21**, 1357 (1981).
15. A. W. Snyder and W. H. Miller, *J. Opt. Soc. Am.* **67**, 5 (1977).
16. We thank F. de Monasterio, W. Makous, S. Schein, B. Thompson, and J. Yellott for valuable discussions. Supported by grants EY 04367 and EY 01319 from the National Eye Institute and an equipment gift from Xerox Corporation.

14 March 1983

Macroevolutionary Trends: New Perspectives on the Roles of Adaptation and Incidental Effect

Abstract. *Trends, long-term directional tendencies in evolution, are traditionally interpreted as selected for and adaptive. Alternatively, trends may be unselected effects of characters and processes within species: the effect hypothesis. Thus adaptations of organisms, varying among species, were selected for immediate fitness, but they may also incidentally determine different speciation and extinction rates and trends.*

A new concept of how the long-term patterns of evolution such as trends may come about, the effect hypothesis (*1*), focuses on a neglected potential of some characters and processes at genomic and organismal levels: the potential to determine differences among related lineages in net species increase. It suggests that differential species diversification and directional phenotypic trends in monophyletic groups (*2*) of sexually reproducing organisms may be nonrandom and yet not adaptive—that is, a particular trend need not be more adaptive, progressive, or successful than alternatives, although all evolution in component lineages may have been under the control of natural selection. In proposing direct upward causation (*3*) to deterministic sorting among species, and therefore to nonadaptive long-term patterns, the effect hypothesis differs from other models of macroevolution, such as the traditional synthetic concept (*4*), the species selection (*5–8*) and random (*9*) models, and the notion that trends are determined largely by intrinsically directed introduction of phenotypic variation (*10*).

Two aspects of trend evolution in monophyletic groups are (i) phenotypic divergence between early and late lineage end points and (ii) the differential increase in numbers of species. The net rate of increase in species in a monophyletic group R is $S - E$, where S is speciation rate and E is species extinction rate (*6, 7*); speciation refers only to lineage splitting. Mean divergence XY in particular characters may theoretically occur separately from or together with differential R. Punctuated equilibria (*5*) introduced the notion of linking divergence and diversity, and to the extent that a punctuated pattern predominates in a phylogeny, we cannot extrapolate notions of directional evolution within species to explain a divergence trend. Rather divergence must depend on variation in S, E, speciation direction, or permutations of them. The trend XY can result from a bias in the direction of speciation events (Fig. 1d) or an increase in R (Fig. 1h). In contrast, divergence trends evolved by "phyletic gradualism" (*5*) are not a function of S and E (Fig. 1, c and g). Punctuated equilibria forces us to consider not only the potential causes of origin and sorting of variation at the level of organismal phenotypes but also those among species. In the absence of a punctuated pattern we still need to explain differential species diversity.

Williams (*11*) suggested that adaptations of organisms, shaped by natural selection to perform particular functions, may have incidental effects that are not the direct consequence of selection. As explicitly argued (*12*) and generally accepted (*13*), speciation is usually an incidental consequence of the accumulation of genotypic and phenotypic differences between populations. To the extent that evolution is about the maintenance of adaptation (*11*), the environmental events that cause speciation may be seen as random accidents, the divergence away from a common fertilization system as disruption, relative to the existing adaptations in the parent species. Thus species are not adaptations, although the component organisms may be adapted, but effects (*12, 14*).

If species commonly result as effects of evolution at lower levels, then it is probable that differential S does as well. If there are characters of genomes and organisms that confer characteristic probabilities of speciation and if such characters in related species differ, then S will differ. Combinations of S and E may vary across a monophyletic group to cause trends toward higher R (Fig. 1, e–h). Suggestions of characters, adaptations, or others, which could potentially effect differential R, focus on susceptibility to new genomic and phenotypic vari-

Consequences of spatial sampling by a human photoreceptor mosaic

DR Williams and R Collier

Science **221** (4608), 385-387.
DOI: 10.1126/science.6867717